Journal of Proteomics 142 (2016) 24–32

Contents lists available at ScienceDirect

Journal of Proteomics

journal homepage: www.elsevier.com/locate/jprot

Global-scale profiling of differential expressed lysine acetylated proteins in colorectal cancer tumors and paired liver metastases

Zhanlong Shen [a,1], Bo Wang [a,1], Jianyuan Luo [b], Kewei Jiang [a], Hui Zhang [a], Harri Mustonen [c], Pauli Puolakkainen [c], Jun Zhu [d], Yingjiang Ye [a,*], Shan Wang [a,*]

[a] Department of Gastroenterological Surgery, Peking University People's Hospital, Beijing 100044, PR China
[b] Department of Medical Genetics, Peking University Health Science Center, Beijing 100191, PR China
[c] Department of Surgery, Helsinki University Central Hospital and University of Helsinki, Helsinki 00290, Finland
[d] Jingjie PTM Biolab (Hangzhou) Co. Ltd, Hangzhou 310018, PR China

ARTICLE INFO

Article history:
Received 25 May 2015
Received in revised form 14 April 2016
Accepted 3 May 2016
Available online 10 May 2016

Keywords:
Lysine acetylation
PTMs
Colorectal cancer
Liver metastasis

ABSTRACT

Lysine acetylated modification was indicated to impact colorectal cancer (CRC)'s distant metastasis. However, the global acetylated proteins in CRC and the differential expressed acetylated proteins and acetylated sites between CRC primary and distant metastatic tumor remains unclear. Our aim was to construct a complete atlas of acetylome in CRC and paired liver metastases. Combining high affinity enrichment of acetylated peptides with high sensitive mass spectrometry, we identified 603 acetylation sites from 316 proteins, among which 462 acetylation sites corresponding to 243 proteins were quantified. We further classified them into groups according to cell component, molecular function and biological process and analyzed the metabolic pathways, domain structures and protein interaction networks. Finally, we evaluated the differentially expressed lysine acetylation sites and revealed that 31 acetylated sites of 22 proteins were downregulated in CRC liver metastases compared to that in primary CRC while 40 acetylated sites of 32 proteins were upregulated, of which HIST2H3AK19Ac and H2BLK121Ac were the acetylated histones most changed, while TPM2 K152Ac and ADH1B K331Ac were the acetylated non-histones most altered. These results provide an expanded understanding of acetylome in CRC and its distant metastasis, and might prove applicable in the molecular targeted therapy of metastatic CRC.

Biological significance: This study described provides, for the first time, that full-scale profiling of lysine acetylated proteins were identified and quantified in colorectal cancer (CRC) and paired liver metastases. The novelty of the study is that we constructed a complete atlas of acetylome in CRC and paired liver metastases. Moreover, we analyzed these differentially expressed acetylated proteins in cell component, molecular function and biological process. In addition, metabolic pathways, domain structures and protein interaction networks of acetylated proteins were also investigated. Our approaches shows that of the differentially expressed proteins, HIST2H3AK19Ac and H2BLK121Ac were the acetylated histones most changed, while TPM2 K152Ac and ADH1B K331Ac were the acetylated non-histones most altered. Our findings provide an expanded understanding of acetylome in CRC and its distant metastasis, and might prove applicable in the molecular targeted therapy of metastatic CRC.

1. Introduction

Colorectal cancer (CRC) is the third most common cancer in the world, with nearly 1.4 million new cases diagnosed in 2012 [1]. In 2014, an estimated 71,830 men and 65,000 women will be diagnosed with colorectal cancer and 26,270 men and 24,040 women will die of the disease [2]. The invasion and distant metastasis were the major determinants of worse prognosis of colorectal cancer [3]. Recently, accumulative novel antitumor drugs were developed to inhibit the advanced cancer progression, especially the molecular targeted drugs [4–8]. However, the overall response rate of most current molecular targeted drugs to the treatment for colorectal cancer was less than 50% [9,10]. Further, side effects are one of the issues of concern [11]. Thus, new targeted molecules of colorectal cancer still need to be investigated. Evidence showed that protein acetylation might be a candidate of therapeutic targets for cancer [12,13]. Epigenetic alteration which leads to modified gene expression was involved in colorectal cancer, initially and during progression [14–16]. Protein acetylation including histone and non-histone proteins, such as transcriptional factors, has been shown to play an important role in the epigenetic regulation of various cancers, and exhibited tissue specificity [12,17,18]. Mutation and/or aberrant expression of various histone deacetylase (HDAC) have also been observed in human disease, in particular cancer, making them a

* Corresponding authors.
E-mail addresses: yeyingjiang@pkuph.edu.cn (Y. Ye), shanwang60@sina.com (S. Wang).
[1] Zhanlong Shen and Bo Wang contributed equally to this work.

http://dx.doi.org/10.1016/j.jprot.2016.05.002
1874-3919/

candidate of therapeutic targets for many human cancers [13]. Histone deacetylase inhibitors (HDIs) have emerged as promising cancer therapeutic agents. To date, two HDIs have been approved for cancer therapy (cutaneous T-cell lymphoma); vorinostat (SAHA, Zolinza) and romodepsin (FK228, Istodax) by the Food and Drug Administration (FDA) [19]. Therefore, targeting protein acetylation represents a potentially promising strategy for human cancers. However, there is no information about the target of acetylation in the colorectal cancer treatment. The main reason is that the critical acetylated protein and site remains unclear in the colorectal cancer.

Proteomic methods are largely based on the use of mass spectrometry (MS), a highly specific, effective, and universal technique that does not require complicated multi-step sample preparation [20]. Proteomics analyses the composition, amounts, isoforms, and posttranslational modifications of cellular proteins [21]. Karczmarski and colleagues [22] used MS-based analysis to quantify global alterations of histone post-translational modifications (PTMs) in normal and colon cancer samples and showed that histone H3 lysine 27 acetylation (H3K27Ac) was associated with colon cancer. However, the differentially expressed acetylated proteins and acetylated sites between CRC primary and distant metastatic tumor remain unclear. In this study, we used integrated approach involving tandem mass tag (TMT) labeling and mass spectrometry-based quantitative proteomics to quantify dynamic changes of protein acetylation including histone or non-histone proteins between matched colon cancer primary and liver metastatic tumor samples. It might throw a new light on the metastatic CRC molecular targeted treatment.

2. Materials and methods

2.1. Patient tissue samples

Three paired colon cancer tissue samples and liver metastases samples (three biological replicates) were obtained from patients undergoing coloproctectomy and immediately snap-frozen and stored at −80 °C until protein extraction. All samples were observed by two pathologists independently and identified as colorectal adenocarcinoma or metastatic cancer. All patients provided written informed consent before samples were collected. The study was approved by the local Research Ethics Committee of Peking University.

2.2. Crude protein extraction

The tissues were first grinded by liquid nitrogen and the powder was transferred to 50 mL centrifuge tube and precipitated with cold 10% TCA/acetone supplemented with 50 mM DTT, 0.1% Protease Inhibitor Cocktail Set IV for 2 h at −20 °C. After centrifugation at 20,000 g at 4 °C for 10 min, the supernatant was discarded. The remaining precipitate was washed with cold acetone supplemented with 50 mM DTT, 1 mM PMSF for three times. After air drying, the precipitate was resuspended in lysis buffer (8 M urea, 2 mM EDTA, 10 mM DTT). The sample was sonicated three times on ice using a high intensity ultrasonic processor (Scientz). The remaining debris was removed by centrifugation at 20,000 g at 4 °C for 10 min. The quality control of the extracted proteins was done by SDS-PAGE (Supplementary Fig. S1).

2.3. Trypsin digestion

For trypsin digestion, the supernatant was transferred to a new tube, reduced with 10 mM DTT for 1 h at 56 °C and alkylated with 55 mM IAA for 45 min at room temperature in darkness. The protein was precipitated with 3 volumes of prechilled acetone for 30 min at −20 °C. After centrifugation, the pellet was then dissolved in 0.5 M TEAB and sonicated for 5 min. The centrifugation step was repeated and the supernatant collected. Protein content was determined with 2-D Quant kit (GE Healthcare) according to the manufacturer's instructions. The protein from each sample was then digested with trypsin overnight at 37 °C in a 1:50 trypsin-to-protein mass ratio.

2.4. Tandem mass tag (TMT) protein labeling

A total of 7.5 mg proteins were digested for enrichment (1.25 mg per plex TMT reagent and 6-plex TMT reagent was used). After trypsin digestion, peptide was desalted by Strata X C18 SPE column (Phenomenex) and vacuum-dried. Peptide was reconstituted in 0.5 M TEAB and processed according to the manufacturer's protocol for 6-plex TMT kit (Thermo). Briefly, one unit of TMT reagent (defined as the amount of reagent required to label 1.25 mg of protein) were thawed and reconstituted in ACN. The peptide mixtures were then pooled and incubated for 2 h at room temperature, desalted and dried by vacuum centrifugation. The six samples of 1 T, 1 M, 2 T, 2 M, 3 T and 3 M were labeled with TMT tag of 126, 127, 128, 129, 130 and 131, respectively.

2.5. Affinity enrichment

To enrich lysine acetylated peptides, tryptic peptides dissolved in NETN buffer (100 mM NaCl, 1 mM EDTA, 50 mM Tris-HCl, 0.5% NP-40, pH 8.0) were incubated with pre-washed antibody beads (purchased PTM Biolabs, Hangzhou, China, Cat. Number PTM-104, it is a mixture of rabbit-derived polyclonal and mouse-derived monoclonal anti-acetyllysine antibodies) at 4 °C overnight with gentle shaking. The beads were washed four times with NETN buffer and twice with ddH_2O. The bound peptides were eluted from the beads with 0.1% TFA. The eluted fractions were combined and vacuum-dried. The resulting peptides were cleaned with C18 ZipTips (Millipore) according to the manufacturer's instructions, followed by analyzing by LC-MS/MS.

2.6. LC-MS/MS analysis

Peptides were dissolved in 0.1% FA (solvent A), directly loaded onto a reversed-phase pre-column (Acclaim PepMap 100, Thermo Scientific, 75 μm × 2 cm, 3 μm, 100 Å). Peptide separation was performed using a reversed-phase analytical column (Acclaim PepMap RSLC, Thermo Scientific, 50 μm × 15 cm, 2 μm, 100 Å). The elution was performed with a linear gradient of 5% ~ 35% solvent B (0.1% FA in 98% ACN) for 30 min and 35% ~ 80% solvent B for 10 min at a constant flow rate of 300 nL/min on an EASY-nLC 1000 UPLC system. The resulting peptides were analyzed by Q Exactive TM Plus hybrid quadrupole-Orbitrap mass spectrometer (Thermo Fisher Scientific).

The peptides were subjected to nanospray ionization (NSI) source followed by tandem mass spectrometry (MS/MS) in Q Exactive (Thermo) coupled online to the UPLC. Intact peptides were detected in the Orbitrap at a resolution of 70,000. The collision mode for acquiring fragment ions is HCD. Peptides were selected for MS/MS using 27% normalized collision energy (NCE) with 12% stepped NCE; ion fragments were detected in the Orbitrap at a resolution of 17,500. The mass window for precursor ion selection is set as 2.0 *m/z*. A data-dependent procedure that alternated between one MS scan followed by 20 MS/MS scans was applied for the top 20 precursor ions above a threshold ion count of 3E4 in the MS survey scan with 15.0 s dynamic exclusion. The electrospray voltage applied was 1.8 kV. Automatic gain control (AGC) was used to prevent overfilling of the Orbitrap; 1E5 ions were accumulated for generation of MS/MS spectra. For MS scans, the *m/z* scan range was 350 to 1600 Da. The fixed first mass was set at 100 *m/z* for TMT quantification.

2.7. Database search

The resulting MS/MS data were processed using MaxQuant with integrated Andromeda search engine (Version 1.4.1.2). TMT were searched against Uniprot_human database (20,274 protein sequences,

released in 11-Dec-2013) with reverse decoy database. Trypsin/P was specified as cleavage enzyme allowing up to 3 missing cleavages, 4 modifications per peptide and 5 charges. Mass error was set to 10 ppm for precursor ions and 0.02 Da for fragment ions. Carbamidomethylation on Cys was specified as fixed modification, oxidation on Met and acetylation on Lys were specified as variable modifications. Reporter ion was set as 6plexTMT for quantification. False discovery rate (FDR) thresholds for protein, peptide and modification site were specified at 1%. Minimum peptide length was set at 6. The other parameters for Maxquant were also follows: min. score for modified peptides is set at 40, min. delta score for modified peptides is set at 17, min. ratio count for protein quantification is 2, min. peptides for identification is 1, site quantification mode is set as use least modified peptide and use normalized ratios, peptide for quantification is set as unique + razor.

2.8. Wilcoxon rank-sum test analysis

Wilcoxon rank-sum test was used to evaluate if the differential expression level of acetylated proteins in one paired tissues was not significantly different from the other two. $P < 0.05$ was considered to be statistically significant.

2.9. Annotation methods

2.9.1. Gene Ontology (GO) annotation

The Gene Ontology is a major bioinformatics initiative to unify the representation of gene and gene product attributes across all species. GO annotation proteome was derived from the UniProt-GOA database (www. http://www.ebi.ac.uk/GOA/). Firstly, Converting identified protein ID to UniProt ID and then mapping to GO IDs by protein ID. If some identified proteins were not annotated by UniProt-GOA database, the InterProScan (http://www.ebi.ac.uk/interpro/, v.5.14-53.0) soft would be used to annotated protein's GO functional based on protein sequence alignment method. Then proteins were classified by Gene Ontology annotation based on three categories: biological process, cellular component and molecular function.

2.9.2. Domain annotation

Identified proteins domain functional description were annotated by InterProScan (http://www.ebi.ac.uk/interpro/, v.5.14-53.0) based on protein sequence alignment method, and the InterPro domain database was used. InterPro (http://www.ebi.ac.uk/interpro/, v.5.14-53.0) is a database that integrates diverse information about protein families, domains and functional sites, and makes it freely available to the public via Web-based interfaces and services.

2.9.3. KEGG pathway annotation

Kyoto Encyclopedia of Genes and Genomes (KEGG) database was used to annotate protein pathway. Firstly, using KEGG online service tools KAAS to annotated protein's KEGG database description. Then mapping the annotation result on the KEGG pathway database using KEGG online service tools KEGG mapper.

2.9.4. Subcellular localization

Wolfpsort (http://www.genscript.com/psort/wolf_psort.html, v.0.2) a subcellular localization predication soft was used to predict subcellular localization of eukaryotic sequences.

2.10. Enrichment analysis method

Differentially expressed Protein functional enrichment analysis shows the functional terms which the differentially expressed lysine acetylated proteins enriched in all quantitative proteins. It represents the important or typical biology functions in the project. In differentially expressed protein enrichment analysis, we used Fisher's exact test method to get the enriched functional terms. We define a differentially expressed protein to be significantly regulated if the p-value is <0.05. Fisher's exact test is a statistical significance test used in the analysis of contingency tables. The test is useful for categorical data that result from classifying objects in two different ways; it is used to examine the significance of the association (contingency) between the two kinds of classification.

2.11. Enrichment-based clustering analysis

All the acetylated substrates categories obtained after enrichment were collated along with their P values, and then filtered for those categories which were at least enriched in one of the clusters with P value < 0.05. This filtered P value matrix was transformed by the function $x = -\log10$ (P value). Finally, these x values were z-transformed for each category. These z scores were then clustered by one-way hierarchical clustering (Euclidean distance, average linkage clustering) in Genesis. Cluster membership was visualized by a heat map using the "heatmap.2" function from the "gplots" R-package.

2.12. Protein-protein interaction analysis

Kac proteins identified were searched against the STRING (http://string-db.org/) database version 10.0 for protein-protein interactions. Only interactions between the proteins contained in the searched data set were selected. STRING (http://string-db.org/) defines a metric called "confidence score" to define interaction confidence: interactions are fetched when a confidence score ≥ 0.7 (high confidence) is reached. Interaction network form STRING was visualized in Cytoscape (http://www.cytoscape.org/v.3.2.1).

3. Results

3.1. Quality control validation of MS data

The MS data validation was shown in Supplementary Fig. S2. Firstly, we checked the mass error of all the identified peptides. The distribution of mass error is near zero and most of them are <2 ppm which means the mass accuracy of the MS data fit the requirement (Supplementary Fig. S2A). Secondly, the length of most peptides distributed between 7 and 13, which agree with the property of tryptic peptides (Supplementary Fig. S2B), that means sample preparation reach the standard.

3.2. Quantification overview of acetylated sites and proteins

In total, 603 acetylation sites from 316 proteins were identified, among which 462 acetylation sites corresponding to 243 proteins were quantified. All the quantified proteins were annotated as shown in Supplementary Table S1 and Supplementary Table S2. More importantly, a crosscheck with the Acetylation-site-dataset of PhosphoSitePlus [23] database revealed that 29 novel acetylated proteins and 228 novel acetylated sites were identified on human beings in this study (Fig. 1A–B).

3.3. Protein annotation

The differentially expressed lysine acetylation sites were also annotated as shown in Table 1 and Table 2 when setting the criteria of >1.3 or <0.769 as up-regulation or down-regulation of lysine acetylation site. Our results showed that, 31 acetylated sites of 22 proteins were down-regulated in all the 3 cases of CRC liver metastases compared to that in CRC primary tissues while 40 acetylated sites of 32 proteins were upregulated (Fig. 1C). Then, we used Wilcoxon rank sum test to analyze if the differential expression level of acetylated proteins in one paired tissues differ from others. The results showed there were no significant differences among the 3 paired tissues ($P = 0.49$). Among the differentially expressed acetylated histone proteins between colorectal primary and

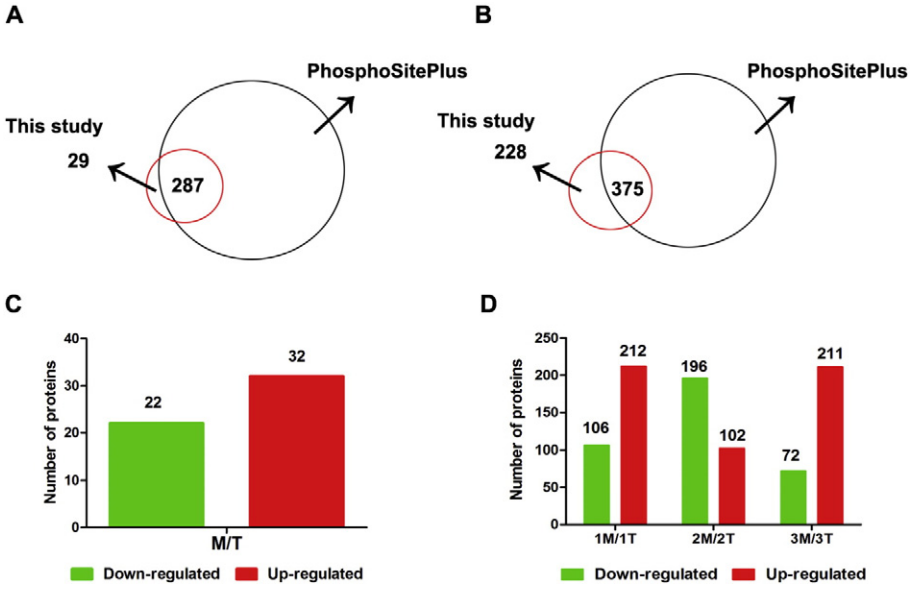

Fig. 1. Distribution of differentially expressed proteins. (A) Comparison of overlapped acetylated proteins between this study and PhosphoSitePlus. Values are number of proteins (B) Comparison of overlapped acetylated sites between this study and PhosphoSitePlus. (C) Differentially expressed acetylated proteins between CRC liver metastases and CRC primary tissues integrated all 3 paired data. (D) Differentially expressed acetylated proteins in each paired metastasis and primary tissues.

Table 1
Differentially expressed acetylation sites obtained in 3 paired samples (Up-regulated).

Protein	Protein description	Kac position	M-vs-T Kac mean ratio	P value	M-vs-T mean ratio	P′ value
Q99880	Histone H2B type 1-L OS = Homo sapiens GN = HIST1H2BL PE = 1 SV = 3	121	7.38	4.08E-02		
P00325	Alcohol dehydrogenase 1B OS = Homo sapiens GN = ADH1B PE = 1 SV = 2	331	3.81	4.24E-02	1.97	6.97E-02
P00367	"Glutamate dehydrogenase 1, mitochondrial OS = Homo sapiens GN = GLUD1 PE = 1 SV = 2"	84	3.71	1.33E-01	1.68	1.41E-02
P05787	"Keratin, type II cytoskeletal 8 OS = Homo sapiens GN = KRT8 PE = 1 SV = 7"	101	3.49	1.28E-01	0.84	2.96E-09
P04406	Glyceraldehyde-3-phosphate dehydrogenase OS = Homo sapiens GN = GAPDH PE = 1 SV = 3	254	3.47	8.45E-02	0.98	1.36E-01
P11142	Heat shock cognate 71 kDa protein OS = Homo sapiens GN = HSPA8 PE = 1 SV = 1	71	3.41	5.99E-03	0.92	3.43E-05
P00325	Alcohol dehydrogenase 1B OS = Homo sapiens GN = ADH1B PE = 1 SV = 2	340	3.11	7.44E-02	1.97	6.97E-02
P00966	Argininosuccinate synthase OS = Homo sapiens GN = ASS1 PE = 1 SV = 2	58	3.07	6.36E-02	1.25	4.40E-07
P61604	"10 kDa heat shock protein, mitochondrial OS = Homo sapiens GN = HSPE1 PE = 1 SV = 2"	8	3.03	1.26E-01	0.82	1.49E-01
O75874	Isocitrate dehydrogenase [NADP] cytoplasmic OS = Homo sapiens GN = IDH1 PE = 1 SV = 2	224	2.91	2.87E-02	1.24	9.35E-02
P02647	Apolipoprotein A-I OS = Homo sapiens GN = APOA1 PE = 1 SV = 1	130	2.78	2.40E-02	1.15	4.22E-03
P02768	Serum albumin OS = Homo sapiens GN = ALB PE = 1 SV = 2	160	2.77	8.13E-02	1.36	3.25E-12
P04004	Vitronectin OS = Homo sapiens GN = VTN PE = 1 SV = 1	275	2.60	6.64E-02	1.72	1.06E-05
P12109	Collagen alpha-1(VI) chain OS = Homo sapiens GN = COL6A1 PE = 1 SV = 3	125	2.56	1.55E-02	0.71	1.07E-03
P07237	Protein disulfide-isomerase OS = Homo sapiens GN = P4HB PE = 1 SV = 3	385	2.50	3.07E-02	1.18	1.08E-07
P02763	Alpha-1-acid glycoprotein 1 OS = Homo sapiens GN = ORM1 PE = 1 SV = 1	170	2.49	3.07E-02	1.27	7.83E-03
P02774	Vitamin D-binding protein OS = Homo sapiens GN = GC PE = 1 SV = 1	345	2.33	1.66E-02	1.22	4.17E-09
P62805	Histone H4 OS = Homo sapiens GN = HIST1H4A PE = 1 SV = 2	92	2.24	3.97E-02	1.07	1.43E-02
P02743	Serum amyloid P-component OS = Homo sapiens GN = APCS PE = 1 SV = 2	218	2.24	1.82E-01	1.51	5.29E-02
P02765	Alpha-2-HS-glycoprotein OS = Homo sapiens GN = AHSG PE = 1 SV = 1	124	2.20	4.92E-02	1.24	8.82E-02
P02647	Apolipoprotein A-I OS = Homo sapiens GN = APOA1 PE = 1 SV = 1	118	2.17	6.35E-02	1.15	4.22E-03
Q5VTE0	Putative elongation factor 1-alpha-like 3 OS = Homo sapiens GN = EEF1A1P5 PE = 5 SV = 1	172	2.07	4.42E-02	1.18	5.20E-02
P05787	"Keratin, type II cytoskeletal 8 OS = Homo sapiens GN = KRT8 PE = 1 SV = 7"	285	2.05	5.17E-02	0.84	2.96E-09
P30101	Protein disulfide-isomerase A3 OS = Homo sapiens GN = PDIA3 PE = 1 SV = 4	335	2.02	1.03E-01	1.04	3.18E-01
P12236	ADP/ATP translocase 2 OS = Homo sapiens GN = SLC25A5 PE = 1 SV = 7	92	1.97	1.51E-02	1.01	4.58E-01
P06733	Alpha-enolase OS = Homo sapiens GN = ENO1 PE = 1 SV = 2	406	1.96	1.37E-02	0.92	2.12E-02
P51659	Peroxisomal multifunctional enzyme type 2 OS = Homo sapiens GN = HSD17B4 PE = 1 SV = 3	663	1.96	9.76E-02	1.28	1.60E-02
P04004	Vitronectin OS = Homo sapiens GN = VTN PE = 1 SV = 1	218	1.93	2.03E-02	1.72	1.06E-05
P10809	"60 kDa heat shock protein, mitochondrial OS = Homo sapiens GN = HSPD1 PE = 1 SV = 2"	396	1.90	2.92E-02	1.23	7.33E-09
P07237	Protein disulfide-isomerase OS = Homo sapiens GN = P4HB PE = 1 SV = 3	375	1.77	2.82E-02	1.18	1.08E-07
P02679	Fibrinogen gamma chain OS = Homo sapiens GN = FGG PE = 1 SV = 3	299	1.68	1.12E-01	1.71	7.43E-02
Q9NR19	"Acetyl-coenzyme A synthetase, cytoplasmic OS = Homo sapiens GN = ACSS2 PE = 1 SV = 1"	418	1.66	4.10E-02	1.01	3.90E-01
P21796	Voltage-dependent anion-selective channel protein 1 OS = Homo sapiens GN = VDAC1 PE = 1 SV = 2	224	1.65	5.72E-02	1.07	3.68E-01
P02679	Fibrinogen gamma chain OS = Homo sapiens GN = FGG PE = 1 SV = 3	196	1.65	1.92E-02	1.71	7.43E-02
P05787	"Keratin, type II cytoskeletal 8 OS = Homo sapiens GN = KRT8 PE = 1 SV = 7"	158	1.61	6.13E-02	0.84	2.96E-09
P01042	Kininogen-1 OS = Homo sapiens GN = KNG1 PE = 1 SV = 2	316	1.54	5.97E-02	1.47	1.44E-03
P02787	Serotransferrin OS = Homo sapiens GN = TF PE = 1 SV = 3	668	1.53	3.70E-02	1.32	1.74E-02
P02647	Apolipoprotein A-I OS = Homo sapiens GN = APOA1 PE = 1 SV = 1	164	1.47	1.74E-02	1.15	4.22E-03
P00738	Haptoglobin OS = Homo sapiens GN = HP PE = 1 SV = 1	77	1.46	3.24E-02	1.39	3.40E-12
Q99436	Proteasome subunit beta type-7 OS = Homo sapiens GN = PSMB7 PE = 1 SV = 1	127	1.39	1.30E-03	1.18	6.36E-02

Table 2
Differentially expressed acetylation sites obtained in 3 paired samples (down-regulated).

Protein	Protein description	Kac position	M-vs-T Kac mean ratio	P value	M-vs-T mean ratio	P′ value
P84243	Histone H3.2 OS = Homo sapiens GN = HIST2H3A PE = 1 SV = 3	19	0.23	2.68E-02	1.00	4.70E-01
P84243	Histone H3.2 OS = Homo sapiens GN = HIST2H3A PE = 1 SV = 3	24	0.23	3.72E-02	1.00	4.70E-01
P07951	Tropomyosin beta chain OS = Homo sapiens GN = TPM2 PE = 1 SV = 1	152	0.25	3.17E-02	0.54	5.51E-02
P84243	Histone H3.2 OS = Homo sapiens GN = HIST2H3A PE = 1 SV = 3	10	0.25	1.34E-01	1.00	4.70E-01
P84243	Histone H3.2 OS = Homo sapiens GN = HIST2H3A PE = 1 SV = 3	15	0.25	1.34E-01	1.00	4.70E-01
P84243	Histone H3.3 OS = Homo sapiens GN = H3F3A PE = 1 SV = 2	28	0.26	9.20E-02	1.00	4.70E-01
P35749	Myosin-11 OS = Homo sapiens GN = MYH11 PE = 1 SV = 3	881	0.29	4.18E-02	1.07	1.08E-12
P62805	Histone H4 OS = Homo sapiens GN = HIST1H4A PE = 1 SV = 2	9	0.29	1.33E-01	1.07	1.43E-02
P62805	Histone H4 OS = Homo sapiens GN = HIST1H4A PE = 1 SV = 2	13	0.30	1.56E-01	1.07	1.43E-02
P62805	Histone H4 OS = Homo sapiens GN = HIST1H4A PE = 1 SV = 2	17	0.31	2.00E-01	1.07	1.43E-02
Q71DI3	Histone H3.2 OS = Homo sapiens GN = HIST2H3A PE = 1 SV = 3	28	0.32	1.62E-01		
P21291	Cysteine and glycine-rich protein 1 OS = Homo sapiens GN = CSRP1 PE = 1 SV = 3	112	0.34	1.18E-01	0.94	2.66E-01
Q01995	Transgelin OS = Homo sapiens GN = TAGLN PE = 1 SV = 4	21	0.34	1.44E-01	0.88	4.63E-01
Q99880	Histone H2B type 1-L OS = Homo sapiens GN = HIST1H2BL PE = 1 SV = 3	17	0.35	6.97E-03		
Q99880	Histone H2B type 1-L OS = Homo sapiens GN = HIST1H2BL PE = 1 SV = 3	21	0.35	3.60E-03		
Q99880	Histone H2B type 1-L OS = Homo sapiens GN = HIST1H2BL PE = 1 SV = 3	24	0.36	5.18E-03		
P35579	Myosin-9 OS = Homo sapiens GN = MYH9 PE = 1 SV = 4	540	0.38	6.28E-02	0.82	1.08E-12
Q96JY6	PDZ and LIM domain protein 2 OS = Homo sapiens GN = PDLIM2 PE = 1 SV = 1	282	0.41	2.63E-02		
P19105	Myosin regulatory light chain 12 A OS = Homo sapiens GN = MYL12A PE = 1 SV = 2	149	0.47	7.26E-02		
Q01844	RNA-binding protein EWS OS = Homo sapiens GN = EWSR1 PE = 1 SV = 1	439	0.52	1.72E-02	0.85	5.32E-02
B2RPK0	Putative high mobility group protein B1-like 1 OS = Homo sapiens GN = HMGB1P1 PE = 5 SV = 1	59	0.52	1.07E-01		
P06454	Prothymosin alpha OS = Homo sapiens GN = PTMA PE = 1 SV = 2	103	0.56	3.57E-02	0.46	1.04E-01
P35579	Myosin-9 OS = Homo sapiens GN = MYH9 PE = 1 SV = 4	1352	0.59	8.31E-03	0.82	1.08E-12
P08758	Annexin A5 OS = Homo sapiens GN = ANXA5 PE = 1 SV = 2	76	0.59	2.16E-02	0.72	2.36E-08
P62937	Peptidyl-prolyl cis-trans isomerase A OS = Homo sapiens GN = PPIA PE = 1 SV = 2	44	0.61	1.74E-03	0.79	9.06E-03
P12110	Collagen alpha-2(VI) chain OS = Homo sapiens GN = COL6A2 PE = 1 SV = 4	851	0.64	1.04E-01	0.82	2.05E-01
P51610	Host cell factor 1 OS = Homo sapiens GN = HCFC1 PE = 1 SV = 2	288	0.64	1.17E-01	0.96	3.34E-01
P07355	Annexin A2 OS = Homo sapiens GN = ANXA2 PE = 1 SV = 2	227	0.65	1.72E-02	0.85	2.20E-01
P06753	Tropomyosin alpha-3 chain OS = Homo sapiens GN = TPM3 PE = 1 SV = 2	153	0.68	3.83E-02	0.59	2.88E-02
P08670	Vimentin OS = Homo sapiens GN = VIM PE = 1 SV = 4	235	0.69	6.26E-02	0.66	0
Q9NQW7	Xaa-Pro aminopeptidase 1 OS = Homo sapiens GN = XPNPEP1 PE = 1 SV = 3	287	0.69	7.24E-04	1.07	6.62E-01

metastatic tumors, acetylated histone H3.2 at Lys 19 (HIST2H3AK19Ac) showed the largest degree of downregulation whereas acetylated histone H2B type 1-L at Lys 121 (H2BLK121Ac) was noted for the greatest changes of overexpression in liver metastatic tissues. Additionally, TPM2 K152Ac and ADH1B K331Ac were the acetylated nonhistones of most obvious alterations. More specifically, in No.1 paired tissues 106 of acetylated proteins were downregulated and 212 were upregulated in liver metastasis tissues compared to that in corresponding primary CRC tissues. In No.2 CRC tissue, 196 acetylation proteins had a lower expression level and 102 were overexpressed. Meanwhile, in No.3 CRC tissue, 72 of acetylated proteins had a decreased expression while 211 were ectopic expressed (Fig. 1D).

3.4. Functional annotation of the Lys acetylome in CRC

To gain functional insight into how Lys acetylation may regulate cellular function, we classified the acetylated proteins to different groups according to cell component, molecular function and biological process. The cell component of acetylated proteins was analyzed by GO annotation. The results revealed that acetylated proteins distributed in various kinds of locations, mainly in cell (27.6%), organelles (24%), membrane-enclosed lumen (12.3%), macromolecular complex (11.8%) and membrane (11.2%) (Fig. 2A). Furthermore, in detail, low-expression or overexpression of acetylated proteins in liver metastatic tumors compared to CRC tissues distributed also primarily in cell (28.7% and 26.5%), organelles (25.1% and 22.8%), membrane-enclosed lumen (9.7% and 14%), macromolecular complex (12.3% and 12.0%) and membrane (9.8% and 11.6%) (Supplementary Fig. S3A, D).

The molecular function analysis showed that of 316 acetylated proteins, 44.7% substrates are associated with binding and 28.6% are related to catalytic activity. The others are involved in structural molecule activity, transporter activity, enzyme regulator activity, electron carrier activity, antioxidant activity and so on (Fig. 2B). In liver metastatic tumors, compared to that in primary tissues, under-expressed or overexpressed acetylated proteins were also mainly involved in binding (49.8% and 42.5%) and catalytic activity (21.0% and 31.1%) (Supplementary Fig. S3B, E).

As far as biological process is concerned, the acetylated proteins are allocated to several groups. 15.6% of acetylated proteins are cellular proteins, 12.8% are metabolic proteins and 12.5% are single-organism proteins (Fig. 2C). Meanwhile, downregulated or upregulated acetylated proteins in liver metastatic tissues mainly associated with cellular process (15.3% and 15.3%), metabolic process (11.3% and 13.0%) and single-organism process (12.7% and 12.3%) (Supplementary Fig. S3C, F).

To further understand the acetylated proteins function in CRC, we evaluated the subcellular localization. Our results showed that the acetylated proteins in CRC are mainly localized in cytoplasm (37.9%), nucleus (21.9%), mitochondria (17.7%) and extracellular region (13.0%) (Fig. 2D).

To understand the cellular pathways involving Lys acetylation in CRC and liver metastases, we performed annotation analysis of KEGG pathways. Our data showed that acetylated proteins were widely involved in signaling pathways, including carbon metabolism (9.5%), biosynthesis of amino acids (5.7%), glycolysis/gluconeogenesis (4.3%), tricarboxylic acid (TCA) cycle (2.9%), fatty acid metabolism (2.1%) and so on (Fig. 2E).

3.5. Enrichment and clustering analysis of the Lys acetylation data sets

We focused on the acetylation that reproducibly changes within the three paired samples (Fig. 3A). To further elucidate the cellular function in metastasis of CRC, we tested the data for enrichment in three GO categories: biological process, cell component and molecular function (Fig. 3B). In the biological process category, processes associated with regulation of response to stress and acute-phase response are significantly enriched in metastases upregulated protein cluster (Supplementary

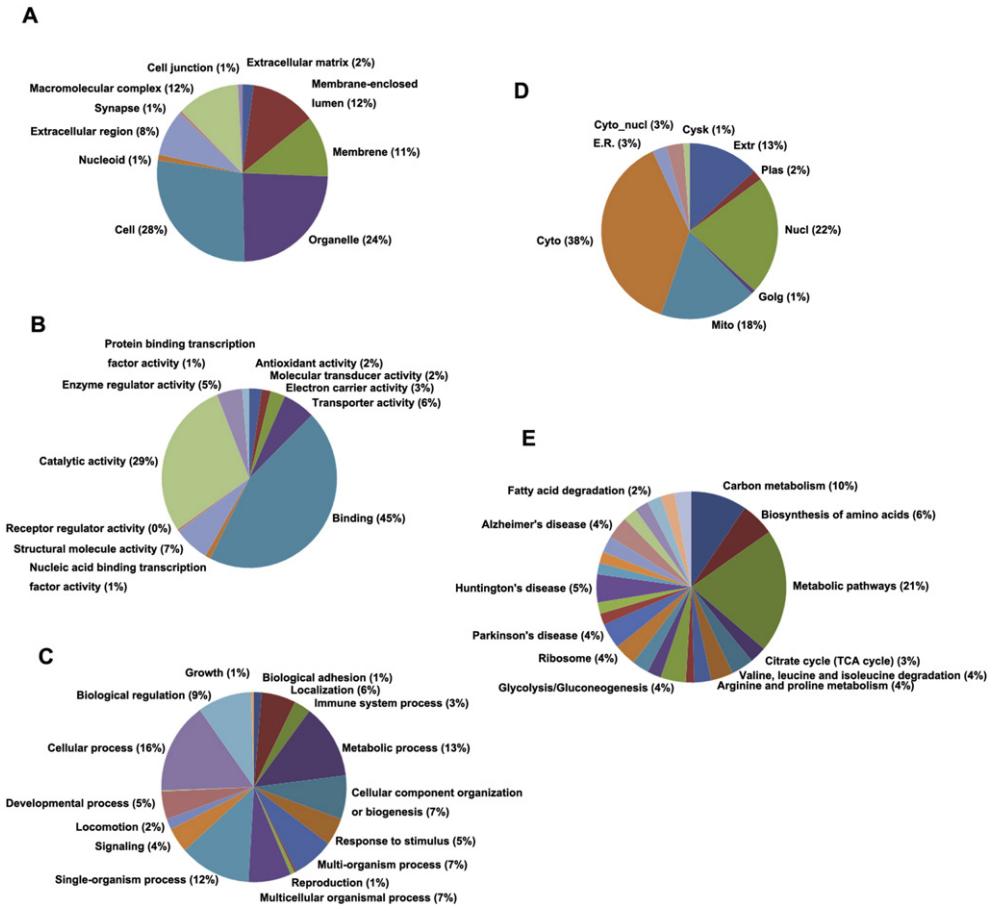

Fig. 2. Characterization of identified acetylated proteins. The classification of acetylated proteins in (A) cell components, (B) molecular function, and (C) biological process. (D) The distribution of acetylated proteins in subcellular localization. (E) The categories of acetylated proteins in KEGG pathways.

Table S3) while chromatin organization and actin filament-based movement are enriched in downregulated proteins (Supplementary Table S4). In agreement with the observation above, the analysis by cellular component revealed that acetylated proteins are enriched mainly in extracellular region and extracellular space in the upregulated proteins while actin filament bundle and stress fiber in the downregulated ones. Furthermore, the evaluation of molecular function showed that proteins involved in DNA binding was enriched in downregulated protein cluster.

Protein functions are largely dependent on specific domain structures in the sequence. To assess the domain structures most regulated between CRC and liver metastases, we performed domain enrichment analysis (Fig. 3C). In agreement with our findings for biological process and cellular component, we revealed that protein domains involved in serum albumin domain was enriched with increased acetylation in CRC liver metastases (Supplementary Table S5) while histone core domain was enriched most in decreased proteins (Supplementary Table S6).

To identify cellular pathways playing great role in CRC, we performed a pathway clustering analysis from KEGG (Fig. 3D). Our data showed that influenza A and legionellosis are the most prominent pathways enriched in metastatic tissues with increased acetylation levels (Supplementary Table S7) and Alcoholism pathway was enriched most in downregulated acetylated proteins (Supplementary Table S8).

3.6. Protein interaction networks of Lys acetylation proteome

We visualized the protein-protein interaction networks of 243 Lys-acetylated proteins on the basis of the STRING database. A complete network of acetylated proteins was created. Our data set offered an insight into the probability of interactions of acetylated proteins in CRC and its liver metastases. A representative example was shown in Fig. 4. Using the MCODE tool [24], we identified some highly connected subnetworks among Lys-acetylated proteins, including ATP synthetase, citrate synthetase, glutathione S transferase and ribosomes. The first two protein networks are localized to mitochondria while the last two are mainly cytosolic.

4. Discussion

Lysine acetylation was first discovered as a post-translational modification of histones in 1964 [25]. During the past few decades, Lys acetylation has been suggested to be an important post-modification in the regulation of the function of both histone and nonhistone proteins [26, 27]. Recently, this modification was indicated to impact CRC's development and progression [28,29]. However, the study of global acetylated proteins has not been performed on CRC, and the number of acetylated proteins is far more than expected due to the limited techniques. Therefore, it is urgent to exclusively investigate the profile of acetylated proteins. In the present study, we used quantitative acetylated proteomics, achieving a global view of acetylome in CRC's primary and liver metastatic tumors. Herein, we identified 603 acetylation sites from 316 proteins, among which 462 acetylation sites corresponding to 243 proteins were quantified. Analysis by combination of all 3 paired tissues indicated that 31 acetylated sites of 22 proteins were downregulated while 40 acetylated sites of 32 proteins were upregulated in liver metastases. This is the first time to reveal the profile of acetylated proteins involved in liver metastasis of CRC. Additionally, in our study, by compared to the acetylation site dataset of PhosphoSitePlus, 228 novel acetylated sites were identified in human, thus expanding the depth of the Lys

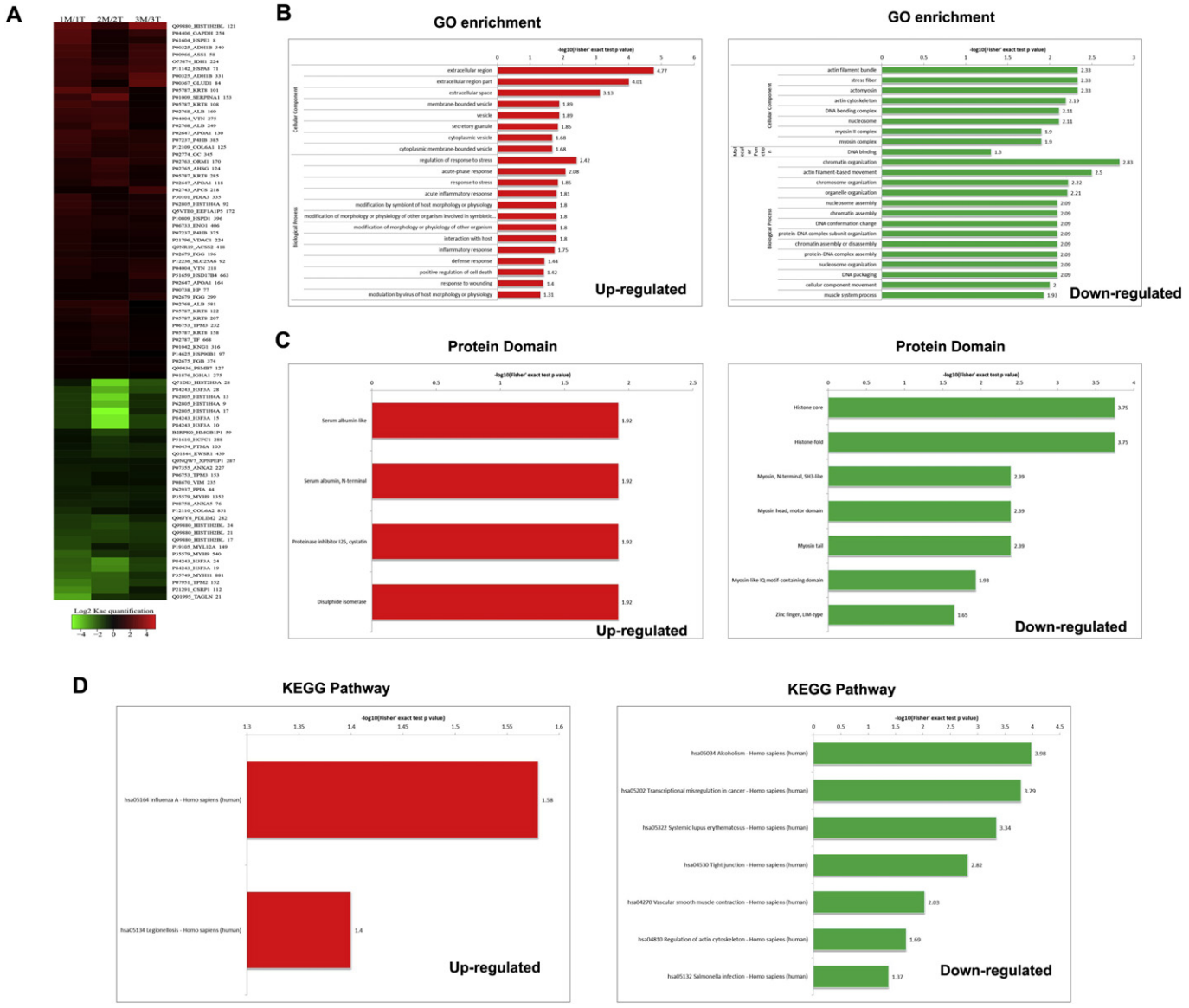

Fig. 3. Enrichment clustering. (A) The enrichment clustering heat map of Lys acetylation that reproducibly changes within the three paired samples. (B) Differential expressed lysine acetylated proteins between liver metastases and primary cancer tissues were classified by GO annotation based on the following three categories: biological process, cellular component, and molecular function. Also, differential expressed lysine acetylated proteins between liver metastases and primary cancer tissues were annotated based on (C) the protein domain database and (D) the KEGG pathway database.

acetylation proteome. This expansion of catalog of acetylated proteins may attribute to the improvement of antibody specificity and recognition range as well as detecting techniques.

To further investigate the characterization of these identified acetylated proteins, we used GO annotation to analyze the potential functions of the acetylated proteins. Our results showed the acetylated proteins of ectopic expression in liver metastases mainly distributed in cell, organelles, macromolecular complex and membrane, functioned largely in molecular binding and catalytic activity, taking part mainly in cellular component and metabolic process. Furthermore, through analysis of KEGG pathway and the protein-interaction networks we discovered that carbon metabolism, biosynthesis of amino acids and TCA cycle are the most prominent pathways enriched in metastatic tissues and the ATP synthetase, citrate synthetase, glutathione S transferase and ribosomes might be the crucial proteins in regulating the process of CRC's metastasis. The profile of acetylated proteins might largely improve our understanding about the role of acetylated proteins plays in metastasis of colorectal tumors.

Among the differentially expressed acetylated histone proteins between colorectal primary and metastatic tumors, acetylated histone H3.2 at Lys 19 (HIST2H3AK19Ac) showed the largest degree of downregulation whereas acetylated histone H2B type 1-L at Lys 121 (H2BLK121Ac) was noted for the greatest changes of overexpression in liver metastatic tissues. A role of histone acetylation is crucial chromatin remodeling for gene transcription since its discovery for the first 30 years [30]. Aberrant acetylation of histones has been indicated to be related to CRC pathogenesis [31]. For example, Fraga et al. revealed that loss of acetylation at Lys16 is a common hallmark in CRC cell lines [32]. Tamagawa et al. observed a low acetylation level of H3K9 in well differentiated colorectal tumors and significantly correlated with tumor histological type [33]. Investigation of global histone acetylation showed that H4K12 and H3K18 exhibited a lower acetylation level in poorly differentiated CRC tissues compared to that of well or moderate differentiated one [34]. Recently, Karczmarski et al. identified H3K27 acetylation as a modification upregulated in CRC by a bottom-up proteomic approach [22]. Based on our present data, we proposed that

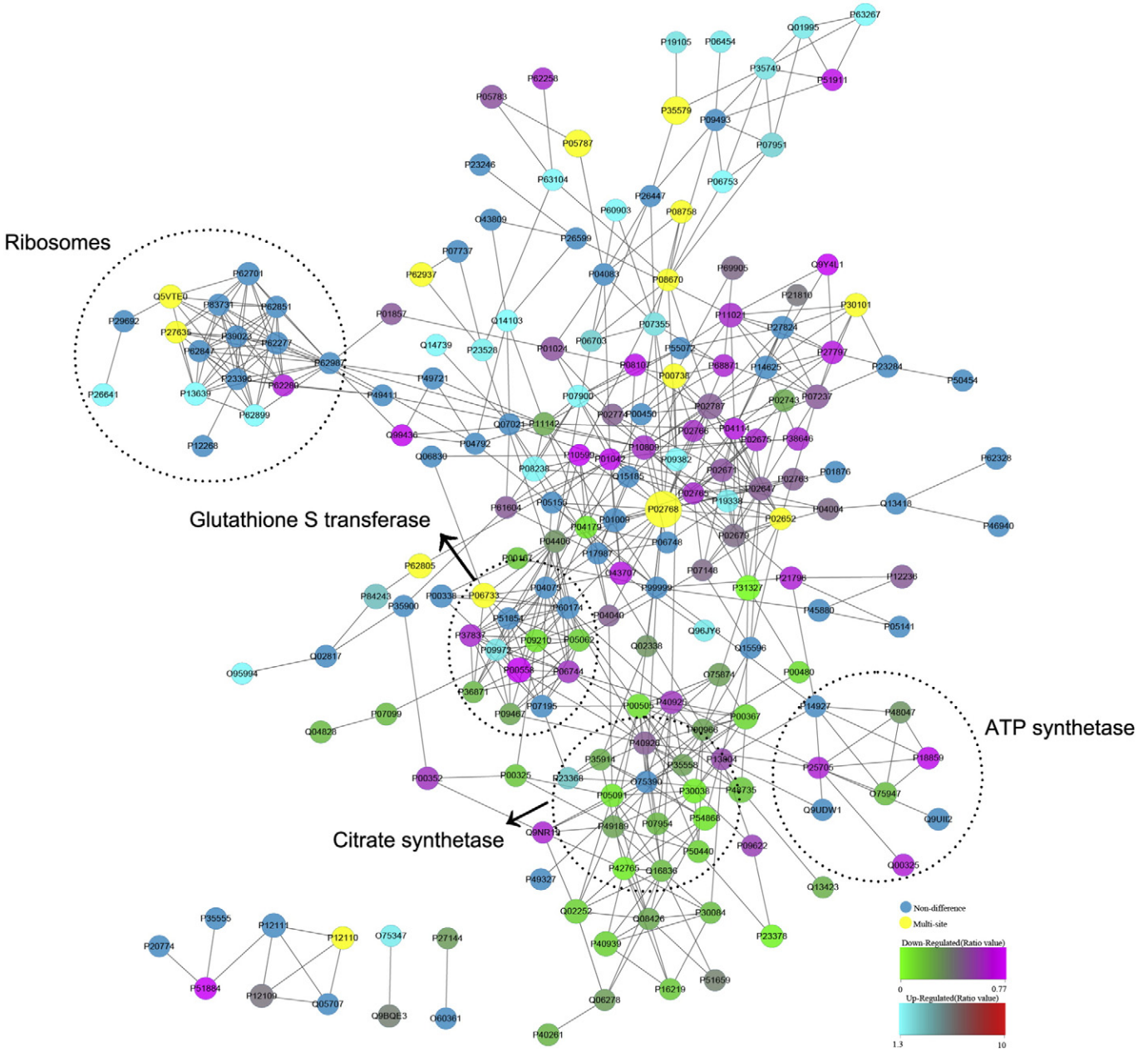

Fig. 4. Representative protein-protein interaction network of Lys acetylation proteome. Interaction networks were analyzed on the basis of the STRING database (v9.1). Some highly connected subnetworks among Lys-acetylated proteins were identified using the MCODE tool.

H4K17Ac and H2BLK121Ac might play a key role in the progress of CRC liver metastasis.

Besides histones acetylation, during the past 30 years, the biological roles of Lys acetylation have been developed in nonhistone proteins [35]. P53 was the first nonhistone protein reported to have potential being modified by acetylation both in vivo and in vitro [36]. In 2006, Kim et al. developed a method to study global protein acetylation and reported about 400 Lys acetylation sites in almost 200 proteins [37]. Soon afterwards, Choudhary et al. identified 3600 acetylation sites on 1750 acetylated proteins, tremendously increasing the size of the acetylome to near that of phosphorylation [38]. In recent years, acetylation of nonhistone proteins was thought to be associated with human cancers. For example, acetylation of HSP90 was indicated to control oncologically relevant proteins in leukemic cells [39]. Acetylation of DBC1 served as a mechanism that connects DNA damage signaling to SirT1 and cell fate determination in lung cancer [40]. Aurora B was regulated by acetylation during mitosis in prostate cancer cells [41]. So far, however, there is still lack of reports about what and how nonhistone acetylation impacts metastasis of CRC based on a tissue-specific proteomics. Our present results have been filling in that blank. We showed that of all differentially expressed acetylated nonhistones, TPM2 K152Ac was the most intensively downregulated protein and ADH1B K331Ac displayed the largest degree of upregulation in liver metastatic tumors. These two acetylated nonhistone proteins might serve as the key regulators contributing to the liver metastasis of CRC.

5. Conclusions

In conclusion, for the first time, combining high affinity enrichment of acetylated proteins with high sensitive mass spectrometry, we identified 603 acetylation sites from 316 proteins in CRC tissues and paired liver metastases, including 29 novel acetylated proteins and 228 novel acetylated sites in human. Therefore, a complete atlas of the acetylome was formed linked to human CRC's liver metastasis. The

characterization of acetylome indicated that acetylated proteins may be pivotal in biological process, protein interaction and metabolic pathways in progress of CRC's metastasis. Furthermore, by comparing differentially acetylated proteins in liver metastases with that of primary cancer tissues, we indicated that 31 acetylated sites of 22 proteins were downregulated while 40 acetylated sites of 32 proteins were upregulated, of which HIST2H3AK19Ac and H2BLK121Ac were the acetylated histones of most intensive changes while TPM2 K152Ac and ADH1B K331Ac were the acetylated nonhistones of most obvious alterations. These results provide us an expanded understanding of acetylome in CRC and its distant metastasis, and might throw a new light on metastatic CRC molecular targeted treatment.

Conflict of interest

The authors declare no competing financial interest.

The following are the supplementary data related to this article.

Supplementary data to this article can be found online at http://dx.doi.org/10.1016/j.jprot.2016.05.002.

Acknowledgments

This study was supported by grants from the National Natural Science Foundation of China (81372290, 81372291) and the Peking University People's Hospital Funds (RDB 2013-15).

References

[1] J. Ferlay, I. Soerjomataram, R. Dikshit, S. Eser, C. Mathers, M. Rebelo, et al., Cancer incidence and mortality worldwide: Sources, methods and major patterns in GLOBOCAN, Int. J. Cancer (2012) 2014.
[2] R. Siegel, C. Desantis, A. Jemal, Colorectal cancer statistics, 2014, CA Cancer J. Clin. 64 (2014) 104–117.
[3] W.M. Boedefeld 2nd, K.I. Bland, M.J. Heslin, Recent insights into angiogenesis, apoptosis, invasion, and metastasis in colorectal carcinoma, Ann. Surg. Oncol. 10 (2003) 839–851.
[4] A. Bonetti, J. Giuliani, F. Muggia, Targeted agents and oxaliplatin-containing regimens for the treatment of colon cancer, Anticancer Res. 34 (2014) 423–434.
[5] M. Kumar, R. Nagpal, R. Hemalatha, V. Verma, A. Kumar, S. Singh, et al., Targeted cancer therapies: the future of cancer treatment, Acta Biomed 83 (2012) 220–233.
[6] J.H. Strickler, H.I. Hurwitz, Bevacizumab-based therapies in the first-line treatment of metastatic colorectal cancer, Oncologist 17 (2012) 513–524.
[7] R.A. de Mello, A.M. Marques, A. Araujo, Epidermal growth factor receptor and metastatic colorectal cancer: insights into target therapies, World J. Gastroenterol. 19 (2013) 6315–6318.
[8] C.M. Hocking, A.R. Townsend, T.J. Price, Panitumumab in metastatic colorectal cancer, Expert. Rev. Anticancer. Ther. 13 (2013) 781–793.
[9] V. Heinemann, P.M. Hoff, Bevacizumab plus irinotecan-based regimens in the treatment of metastatic colorectal cancer, Oncology 79 (2010) 118–128.
[10] J.R. Hecht, E. Mitchell, T. Chidiac, C. Scroggin, C. Hagenstad, D. Spigel, et al., A randomized phase IIIB trial of chemotherapy, bevacizumab, and panitumumab compared with chemotherapy and bevacizumab alone for metastatic colorectal cancer, J. Clin. Oncol. 27 (2009) 672–680.
[11] P. Tappenden, R. Jones, S. Paisley, C. Carroll, Systematic review and economic evaluation of bevacizumab and cetuximab for the treatment of metastatic colorectal cancer, Health Technol. Assess. 11 (2007) 1–128 (iii-iv).
[12] Y. Tang, W. Zhao, Y. Chen, Y. Zhao, W. Gu, Acetylation is indispensable for p53 activation, Cell 133 (2008) 612–626.
[13] B. Barneda-Zahonero, M. Parra, Histone deacetylases and cancer, Mol. Oncol. 6 (2012) 579–589.
[14] B. Zhang, J. Wang, X. Wang, J. Zhu, Q. Liu, Z. Shi, et al., Proteogenomic characterization of human colon and rectal cancer, Nature 513 (2014) 382–387.
[15] H. Ashktorab, K. Belgrave, F. Hosseinkhah, H. Brim, M. Nouraie, M. Takkikto, et al., Global histone H4 acetylation and HDAC2 expression in colon adenoma and carcinoma, Dig. Dis. Sci. 54 (2009) 2109–2117.
[16] H. Tamagawa, T. Oshima, M. Shiozawa, S. Morinaga, Y. Nakamura, M. Yoshihara, et al., The global histone modification pattern correlates with overall survival in metachronous liver metastasis of colorectal cancer, Oncol. Rep. 27 (2012) 637–642.
[17] A. Kuzmichev, R. Margueron, A. Vaquero, T.S. Preissner, M. Scher, A. Kirmizis, et al., Composition and histone substrates of polycomb repressive group complexes change during cellular differentiation, Proc. Natl. Acad. Sci. U. S. A. 102 (2005) 1859–1864.
[18] A. Aghdassi, M. Sendler, A. Guenther, J. Mayerle, C.O. Behn, C.D. Heidecke, et al., Recruitment of histone deacetylases HDAC1 and HDAC2 by the transcriptional repressor ZEB1 downregulates E-cadherin expression in pancreatic cancer, Gut 61 (2012) 439–448.
[19] O. Khan, N.B. La Thangue, HDAC inhibitors in cancer biology: emerging mechanisms and clinical applications, Immunol. Cell Biol. 90 (2012) 85–94.
[20] K. Zhang, S. Zheng, J.S. Yang, Y. Chen, Z. Cheng, Comprehensive profiling of protein lysine acetylation in Escherichia coli, J. Proteome Res. 12 (2013) 844–851.
[21] J. Ostrowski, L.S. Wyrwicz, Integrating genomics, proteomics and bioinformatics in translational studies of molecular medicine, Expert. Rev. Mol. Diagn. 9 (2009) 623–630.
[22] J. Karczmarski, T. Rubel, A. Paziewska, M. Mikula, M. Bujko, P. Kober, et al., Histone *H3* lysine 27 acetylation is altered in colon cancer, Clin. Proteomics 11 (2014) 24.
[23] P.V. Hornbeck, J.M. Kornhauser, S. Tkachev, B. Zhang, E. Skrzypek, B. Murray, et al., PhosphoSitePlus: a comprehensive resource for investigating the structure and function of experimentally determined post-translational modifications in man and mouse, Nucleic Acids Res. 40 (2012) D261–D270.
[24] G.D. Bader, C.W. Hogue, An automated method for finding molecular complexes in large protein interaction networks, BMC Bioinf. 4 (2003) 2.
[25] A. Vg, R. Faulkner, M. Ae, Acetylation and methylation of histones and their possible role in the regulation of RNA synthesis, Proc. Natl. Acad. Sci. U. S. A. 51 (1964) 786–794.
[26] W. Gu, R.G. Roeder, Activation of p53 sequence-specific DNA binding by acetylation of the p53 C-terminal domain, Cell 90 (1997) 595–606.
[27] M. Zheng, J. Zhu, T. Lu, L. Liu, H. Sun, Z. Liu, et al., p300-mediated histone acetylation is essential for the regulation of GATA4 and MEF2C by BMP2 in H9c2 cells, Cardiovasc. Toxicol. 13 (2013) 316–322.
[28] J. Wang, J. Qian, Y. Hu, X. Kong, H. Chen, Q. Shi, et al., ArhGAP30 promotes p53 acetylation and function in colorectal cancer, Nat. Commun. 5 (2014) 4735.
[29] L.T. Wang, J.P. Liou, Y.H. Li, Y.M. Liu, S.L. Pan, C.M. Teng, A novel class I HDAC inhibitor, MPT0G030, induces cell apoptosis and differentiation in human colorectal cancer cells via HDAC1/PKCdelta and E-cadherin, Oncotarget 5 (2014) 5651–5662.
[30] Norris KL, Lee JY, Yao TP. Acetylation goes global: the emergence of acetylation biology. Sci. Signal. 2009; 2:pe76.
[31] A.N. Gargalionis, C. Piperi, C. Adamopoulos, A.G. Papavassiliou, Histone modifications as a pathogenic mechanism of colorectal tumorigenesis, Int. J. Biochem. Cell Biol. 44 (2012) 1276–1289.
[32] M.F. Fraga, E. Ballestar, A. Villar-Garea, M. Boix-Chornet, J. Espada, G. Schotta, et al., Loss of acetylation at Lys16 and trimethylation at Lys20 of histone H4 is a common hallmark of human cancer, Nat. Genet. 37 (2005) 391–400.
[33] H. Tamagawa, T. Oshima, M. Shiozawa, S. Morinaga, Y. Nakamura, M. Yoshihara, et al., The global histone modification pattern correlates with overall survival in metachronous liver metastasis of colorectal cancer, Oncol. Rep. 27 (2012) 637–642.
[34] H. Ashktorab, K. Belgrave, F. Hosseinkhah, H. Brim, M. Nouraie, M. Takkikto, et al., Global histone H4 acetylation and HDAC2 expression in colon adenoma and carcinoma, Dig. Dis. Sci. 54 (2009) 2109–2117.
[35] S. Lee, Post-translational modification of proteins in toxicological research: focus on lysine acylation, Toxicol. Res. 29 (2013) 81–86.
[36] W. Gu, R.G. Roeder, Activation of p53 sequence-specific DNA binding by acetylation of the p53 C-terminal domain, Cell 90 (1997) 595–606.
[37] S.C. Kim, R. Sprung, Y. Chen, Y. Xu, H. Ball, J. Pei, et al., Substrate and functional diversity of lysine acetylation revealed by a proteomics survey, Mol. Cell 23 (2006) 607–618.
[38] C. Choudhary, C. Kumar, F. Gnad, M.L. Nielsen, M. Rehman, T.C. Walther, et al., Lysine acetylation targets protein complexes and co-regulates major cellular functions, Science 325 (2009) 834–840.
[39] O.H. Kramer, S. Mahboobi, A. Sellmer, Drugging the HDAC6-HSP90 interplay in malignant cells, Trends Pharmacol. Sci. 35 (2014) 501–509.
[40] H. Zheng, L. Yang, L. Peng, V. Izumi, J. Koomen, E. Seto, et al., hMOF acetylation of DBC1/CCAR2 prevents binding and inhibition of SirT1, Mol. Cell. Biol. 33 (2013) 4960–4970.
[41] M. Fadri-Moskwik, K.N. Weiderhold, A. Deeraksa, C. Chuang, J. Pan, S.H. Lin, et al., Aurora B is regulated by acetylation/deacetylation during mitosis in prostate cancer cells, FASEB J. 26 (2012) 4057–4067.